Nanoparticle Synthesis

Au nanoparticles (NPs) were carefully synthesized following similar procedures previously reported in literature[1, 2]. First an aqueous solution of $HAuCl_4$ (30 mM, 30 mL) was added to a toluene solution of *n*-tetraoctlyammonium bromide (TOAB, 50 mM, 80 mL) and vigorously stirred at room temperature with a magnetic stirrer for 10 minutes. Using a globe separation funnel, the aqueous solution was discarded and the less dense (reddish-purple) toluene solution was then rinsed three times with 100 mL of de-ionized water. Next, an aqueous solution of sodium borohydride ($NaBH_4$, 400 mM, 25 mL) was added drop-wise to the toluene solution and stirred for one hour using a magnetic stirrer at room temperature. The $NaBH_4$ serves as a reducing agent allowing TOAB ligands to coat Au NPs. After the reaction was complete, the Au-NP-toluene solution was rinsed with 100 mL of de-ionized water (3x), 0.01 M aqueous H_2SO_4 solution (1x), de-ionized water (1x), 0.05 M aqueous Na_2CO_3 solution (1x), and finally with de-ionized water (5x). The NP solution was then dried over Na_2SO_4 for 12 hours before decanting through a filter. The solution was then stored under N_2 shielded from light until use.

The size of the nanoparticles was determined using (i) high-resolution transmission electron microscope (TEM, JEOL 2100) at beam voltage of 200 kV drop cast on a carbon coated TEM grid, (ii) dynamic light scattering (DLS, Viscotek 802), and (iii) UV-vis absorption spectroscopy(Varian/Cary 50 Scan). TEM samples were prepared by depositing one drop of NP solution onto a copper grid using a 0.05 µm filtered syringe and then by allowing the solvent to evaporate. TEM image analysis (Fig. S-1) of >200 particles suggests a mean diameter of 5.73 ± 0.82 nm. DLS and UV-vis absorption sample were prepared by adding five drops of NP solution to 5 mL of anhydrous toluene and loaded into a 1 cm cuvette for analysis. DLS suggests mean diameters of 5.64 ± 0.21 nm and 5.56 ± 0.25 nm on a number density and mass density basis, respectively. UV-vis absorption finds that the plasmon resonance peak is well defined at 525 nm further confirming the size of the nanoparticles.

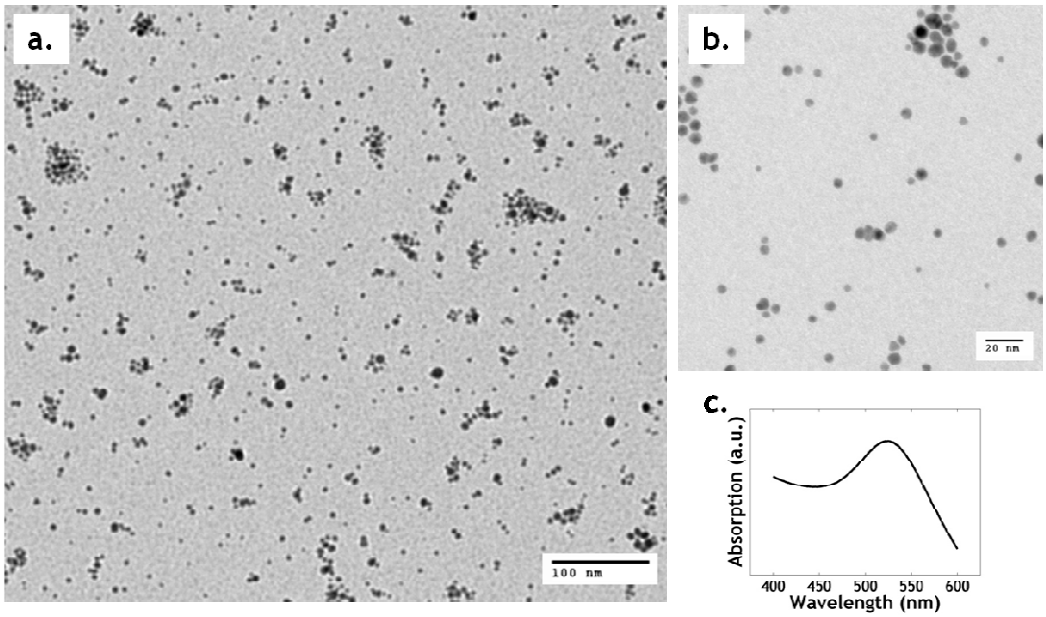

Figure S-1: Au nanoparticles: (a) TEM image of Au nanoparticles at the 100 nm scale, (b) enlarged TEM image of Au nanoparticles at the 20 nm scale, (c) UV-vis absorption spectra of dilute Au nanoparticle solution in toluene with a plasmon resonance peak at 525 nm.

Substrate Preparation

Au substrates were prepared using the template stripped gold technique[3-5] and illustrated in Fig. 2. First, 200 nm of Au was sputtered onto a pristine silicon wafer using an Edwards Auto 306 DC sputter coater with an Ar flow rate of 20 sccm at a power of 200 W without using an adhesion layer. Next, EPO-TEK 377 (Epoxy Technology, Inc.) is prepared following manufacturer's instructions (equal parts by mass) and a single drop is applied to a glass microscope cover slide. The cover slide is then epoxied to the Au-coated silicon wafer with care taken to prevent the glass from directly bonding to the silicon wafer. The glass-epoxy-Au-wafer sandwich is then baked at 150 ºC curing the epoxy. The sandwiches can then be stored for extended periods of time before use. When substrates are desired, a piece of tape is used to mechanically strip the substrate from the silicon template. Substrate characterization was carried out using a Molecular Imaging scanning tunneling microscope (STM) and an RMS roughness of 1.68 ± 0.18 Å over a scan size of 50 x 50 nm was measured over multiple samples. An Asylum MFP-3D atomic force microscope was also used to image the surface and Au plateaus were observed over large scan sizes (1 x 1 µm) (Fig. S-2).

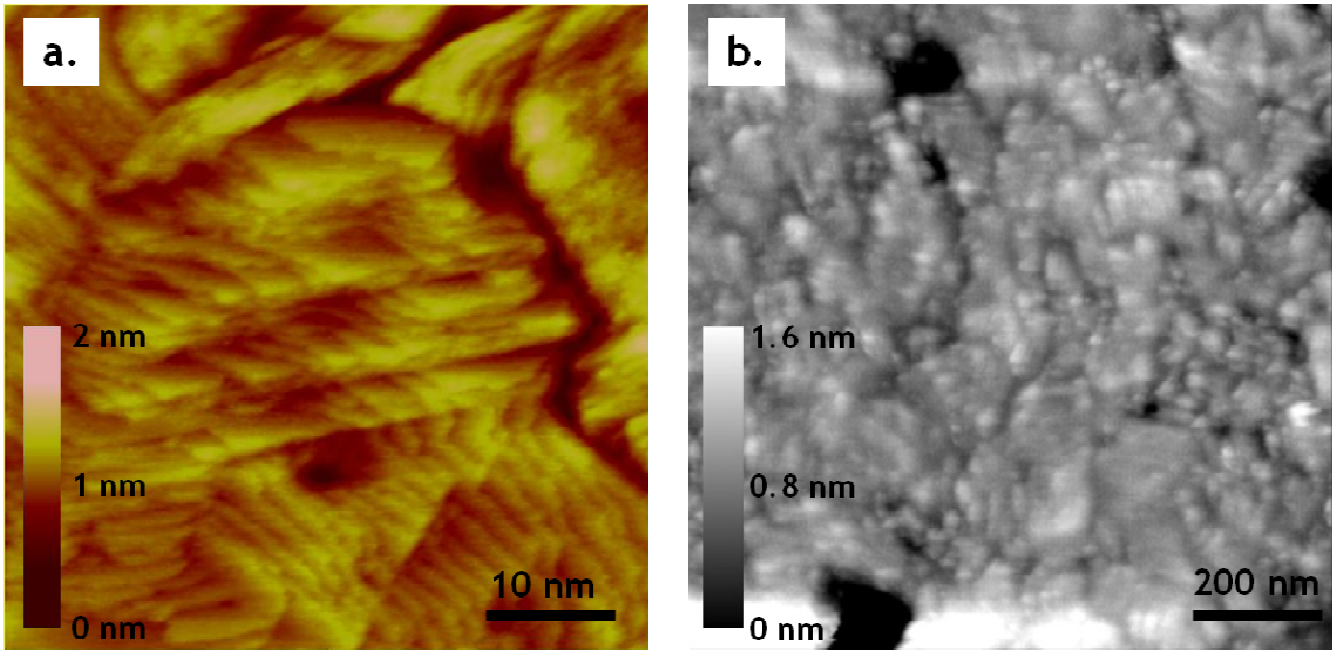

Figure S-2: (a) STM image and (b) AFM image of a Au substrate with RMS roughness of 1.68 ± 0.18 Å showing Au terrace steps over a large area

AFM Tip Preparation

The AFM tips were modified from commercially available Olympus AC240TS silicon AFM cantilevers (spring constant ~2 N/m, tip radius ~9 nm) following the procedure outlined by Morita[1]. A stiffer cantilever was used to prevent snap-in during electrical measurements. Au and Cr where alternatively evaporated in a Veeco 401 vacuum system and thickness was controlled using a crystal monitor: (bottom, first layer) Cr 25 Å – Au 50 Å – Cr 25 Å – Au 50 Å – Cr 25 Å – Au 100 Å – Cr 25 Å – Au 300 Å (top, final layer). Scanning electron microscope (SEM) images with energy dispersive x-ray spectroscopy (EDS) confirm that Au dominates the final layer of deposition (Fig. S-3). These cantilevers appear to be robust over hundreds of approach and withdraw sequences and Au flaking is at a minimum.

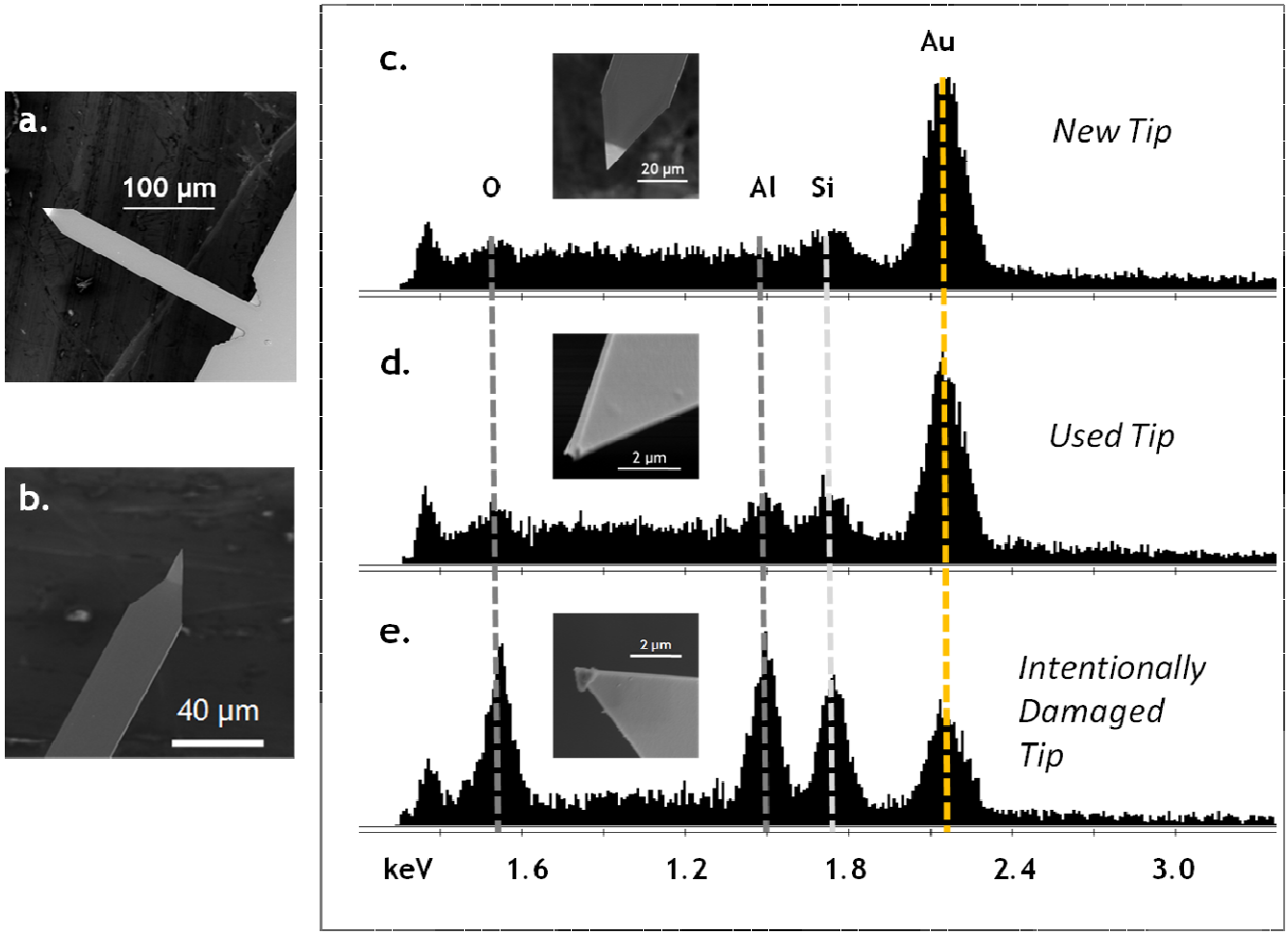

Figure S-3: Modified AFM cantilevers: SEM images of cantilever (a) before and (b) after Au/Cr coating. SEM and EDS of cantilever tip of (c) a new tip before use, (d) a tip after use, and (e) a tip that has intentionally been damaged. The EDS spectrum of the new tip shows that Au x-rays dominate and Cr is not appreciable. Even after use, Au is still present on the tip however x-rays from the underlying silicon and the aluminum (native Al_2O_3) reflective top coat are also visible. A separate tip was intentionally damage by manually scoring it across the sample and the silicon and aluminum x-rays are more visible but some Au still remains.

Molecular Synthesis

All synthesis was performed under a nitrogen atmosphere using standard Schlenk techniques. HPLC-grade solvents were obtained from Fisher Scientific without further purification. ^{1}H and $^{13}C\ \{^{1}H\}$ NMR spectra were recorded at room temperature using Bruker AV-300 MHz or AVB-400 MHz NMR spectrometers. Chemical shifts were measured relative to solvent resonances. Elemental analyses were performed by the Micro-Analytical Laboratory in the College of Chemistry at the University of California, Berkeley. Matrix-Assisted Laser Desorption/Ionization (MALDI) was performed on an Applied Biosystems Voyager MALDI machine with 1,8,9-anthrathenetriol as the matrix. Cyclic voltammetry was performed on a Bioanalytical Systems CV-50W Voltammetric Analyzer with a C-3 Cell Stand. The potentials were measured vs. a $Ag/AgNO_3$ non-aqueous reference electrode, with glassy carbon as the working electrode and a Pt wire axial electrode in a 0.1 M tetrabutylammoniumhexafluorophosphate acetonitrile solution. Ferrocene was used as the external standard (HOMO = -4.8 eV) and the potential sweep rate was 100 mV/s unless otherwise stated.

First, Compound **1** (2,2-bithiophene-5-thiol) was prepared according to literature[6]. Next (as shown in Fig. S-4) Compound **3** was synthesizes by combining Compound **1** (35.0 g, 0.18 mol), $KOBu^t$ (20.8 g, 0.19 mol) and 200 mL THF/CH_3OH (v/v = 1:1) in a 500 mL flask with a reflux condenser. This solution was refluxed for 120 minutes and allowed to cool to room temperature. The solvent was then removed under vacuum leaving 41.0 g of Compound **2** as a yellow solid (98% yield) which was used without further purification. Compound **2** (6.5 g, 27.6 mmol) was then dissolved in 150 mL solution of a CH_3OH and THF (10 mL) before TMSCCBr (5.0 g, 27.6 mmol) was added quickly at 0 °C. The resulting yellowing solution was refluxed overnight. The solvent was then removed and the orange solid was extracted by hexanes; the hexanes were removed and the resulting crude product was passed through a silica gel plug (30 cm). 7.6 grams of a light yellow oil (92% yield) was obtained as a pure product. ^{1}HNMR (300 MHz, $CDCl_3$) δ 0.05 (s, 9H), 0.96 (m, 2 H), 2.90 (m, 2H), 7.05 (m, 3H), 7.21 (t, 1H), 7.25 (d, 1H). ^{13}C NMR (75.5 MHz, $CDCl_3$) δ -1.4, 17.9, 35.6, 124.1, 124.87, 128.2, 134.3, 134.5, 137.4, 140.8. Anal. Calcd for $C_{13}H_{18}S_3Si$: C, 52.30; H 6.08. Found: C, 52.47; H 6.13.

Compound **4** was synthesized by mixing Compound **3** (3.15 g, 10.5 mmol) and NBS (1.88 g, 10.6 mmol) in 30 mL of THF at 0 °C. The solution was stirred at room temperature for 4 hours. The solvent was then removed and the product was purified by a silica gel column with hexanes as the eluent to isolate 3.50 g of Compound **4** as a yellow oil (88% yield). ^{1}HNMR (400 MHz, $CDCl_3$) δ 0.02 (s, 9H), 0.93 (m, 2 H), 2.87 (m, 2H), 6.88 (d, 2H), 6.97 (m, 3H). ^{13}C NMR (75.5 MHz, $CDCl_3$) δ -1.5, 17.6, 34.1, 111.5, 124.1, 124.3, 130.9, 134.1, 135.2, 138.8, 139.5. M.S.: 378.01 (M^+).

Compound **5** was synthesized by mixing Compound **4** (3.20 g, 8.5 mmol), 4-ethynylaniline (1.0 g, 8.5 mmol), $Pd(Ph_3)_2Cl_2$ (0.32 g, 0.46 mmol), CuI (0.16 g, 0.84 mmol), and PPh_3 (0.48 g, 0.92 mmol) together in 100 mL of NEt_3. The solution was de-aired by bubbling N_2 for 30 minutes and stirred at 100 °C for 24 hours. The solvent was then removed under vacuum. The resulting brown solid was extracted with diethyl ether. The solvent was then removed and the crude product was purified by a silica gel column with $CHCl_3$ as the eluent to isolate 2.84 g of Compound **5** (81% yield) as an orange oil. ^{1}HNMR (300 MHz, $CDCl_3$) δ 0.04 (s, 9H), 0.96 (m, 2 H), 2.90 (m, 2H), 3.85 (br, 2H), 6.62 (d, 2H), 7.02 (m, 3H), 7.13 (d, 1H), 7.39 (d, 2H). ^{13}CNMR (75.5 MHz, $CDCl_3$) δ -1.4, 17.9, 35.1, 81.0, 95.8, 112.1, 115.1, 123.3, 123.9, 124.4, 132.3, 133.2, 134.1, 135.1, 137.9, 140.1, 147.4. M.S.: 413.25 (M^+).

Compound **7** was synthesized by mixing Compound **5** (1.0 g, 2.4 mmol) and 1,4,5,8-naphthalene-tetracarboxylic dianhydride (4.0 g, 15.3 mmol) together in 50 mL of DMF. The solution was de-aired by bubbling N_2 for 30 minutes and stirred at 145 °C for 12 hours. The solution was then cooled down and excess 1,4,5,8-naphthalene-tetracarboxylic dianhydride was removed by filtering finally yielding a dark brown solution as Compound **6.** The Compound **6** solution was then mixed with 2-aminoethanethiol (2.0 g, 26.0 mmol). This resulting solution was de-aired by bubbling N_2 for 30 minutes and stirred at 145 °C for another 12 hours. The solvent was then removed under vacuum. The resulting brown solid was purified by using a silica gel column with $CHCl_3$ as the eluent to isolate 0.62 g of Compound **7** (33% yield) as a brown solid. ^{1}HNMR (400 MHz, $CDCl_3$) δ 0.02 (s, 9H), 0.92 (m, 2 H), 1.57 (m, 2H), 2.91 (m, 4H), 3.10 (br, 1H), 6.99 (d, 1H), 7.03 (d, 1H), 7.05 (d, 1H), 7.20 (d, 1H), 7.30 (d, 2H), 7.68 (d, 2H), 8.81 (br, 4H). Anal. Calcd for $C_{37}H_{30}N_2O_4S_4Si$: C, 61.67; H 4.18; N 3.87. Found: C, 61.22; H 4.14; N 3.92. Compound **7**, was the final P-N molecule that was used in experiments.

This robust synthesis produces high yield stable molecules and affords the option of chemically exchanging the different bridges and endgroups for subsequent study. In particular, three other variations were synthesized where an insulating alkane bridge and conducting phenyl endgroups were used. Herein, we only report results from our conducting-bridge insulating-endroup molecule and focus on the measurement techniques and initial findings.

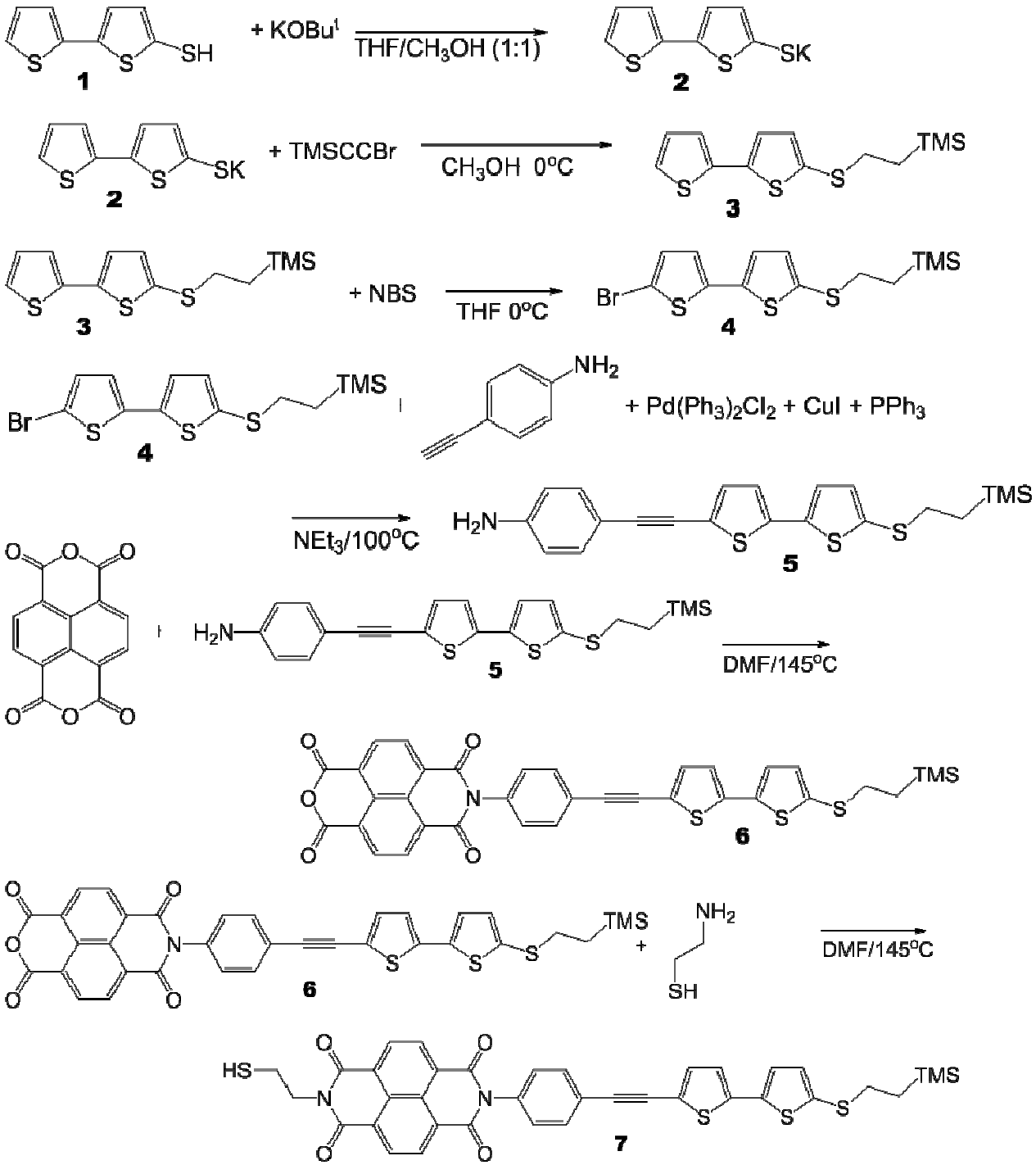

Figure S-4: Synthesis of Compounds **2** through **7**.

DFT/Δ-SCF Calculations

The Δ-SCF method expresses the ionization potential and the electronic affinity of the isolated molecule as a difference in total energies of the anion and cation with respect to the neutral species. Namely the ionization potential (IP) is the difference in energy between the neutral species and one containing one fewer electrons while electronic affinity (EA) is the difference in energy between the neutral species and once containing one more electron. Moreover, in the presence of a metallic surface, the charged excitations polarize the metallic surface, resulting in an image correction energy (IC) that scales as the inverse of distance between the orbital and the image plane of the metal. For a Au (111) surface, we calculated that the image plane lies 1 Å into vacuum with respect to the position of the Au atoms. The image correction energy then effectively reduces the HOMO-LUMO gap of a molecule. The calculation of the HOMO-LUMO gap for the isolated molecule is therefore the difference in ionization potential and electron affinity minus the image charge correction energy (*i.e.*, E_{gap} = IP-EA-IC). In this case, considering different configurations of the molecule between two electrodes separated by 30 Å, this reduction of the band gap is always less than 1.2 eV and the Δ-SCF method based on the B3LYP approximation for the exchange and correlation energy for the molecule in the gas phase gives a gap of 4.45 eV.

Electronic Transport Model

The current is obtained through the Landauer formula as:

$$I\left(V_{1-2}\right)=sign\left(V_{1-2}\right)G_0\int_{-|V_{1-2}|/2}^{+|V_{1-2}|/2}\tau(\omega,E\left(V_{1-2}\right))d\omega \tag{1}$$

where $\pm V_{1-2}/2$ represents the variation of the chemical potentials in the leads, G_0 is the quantum of conductance, and $\tau(\omega,E(V_{1-2}))$ is the transmission function. Next, the transmission function can be approximated by a bias-dependent Lorentzian, where the position of the resonance is given by the function $E(V_{1-2})$:

$$\tau\left(\omega,E\left(V_{1-2}\right)\right)=\frac{4\lambda\Gamma^2}{\left(1+\lambda\right)^2\Gamma^2+4\left(\omega-E\left(V_{1-2}\right)\right)^2} \tag{2}$$

where the coupling of the level to the closest lead is given by Γ and to the furthest lead by $\lambda\Gamma$ where by convention $\lambda<1$. Assuming that Γ and λ do not vary as a function of the bias, which is associated with the absence of variation of the wavefunctions with the bias, and performing the integration analytically, the current is given by:

$$I\left(V_{1-2}\right)=\frac{4\lambda\gamma G_0}{1+\lambda}\left[\boldsymbol{arctan}\left(\frac{V_{1-2}/2+E\left(V_{1-2}\right)}{\gamma\left(1+\lambda\right)}\right)+\boldsymbol{arctan}\left(\frac{V_{1-2}/2-E\left(V_{1-2}\right)}{\gamma\left(1+\lambda\right)}\right)\right] \tag{S-1}$$

where $\gamma=\frac{\Gamma}{2}$. Now assume that:

$$E\left(V_{1-2}\right)=\frac{\alpha}{2}V_{1-2}+E_0 \tag{3}$$

where E_0 represents the position of the molecular orbital at zero-bias. $\alpha=\pm1$ indicates that the level moves rigidly with the chemical potential of an electrode (Tersoff-Hamann limit) while $\alpha=0$ indicates that the energy of the molecular orbital is bias independent. Differentiating with respect to V, one obtains the differential conductance:

$$\begin{aligned}\left.\frac{dI\left(V\right)}{dV}\right|_{V=V_{1-2}}&=\frac{G_0}{2}\left[\tau\left(\frac{-V_{1-2}}{2},E\left(V_{1-2}\right)\right)+\tau\left(\frac{V_{1-2}}{2},E\left(V_{1-2}\right)\right)\right]\\&+\frac{\alpha G_0}{2}\left[\tau\left(\frac{-V_{1-2}}{2},E\left(V_{1-2}\right)\right)-\tau\left(\frac{V_{1-2}}{2},E\left(V_{1-2}\right)\right)\right]\end{aligned} \tag{S-2}$$

The first part of this equation is symmetric with respect to the sign of the bias, and therefore does not contribute to the rectification. The second part is antisymmetric with respect to the applied bias and is non-zero only when $\alpha\neq0$ and $E\left(V_{1-2}\right)\neq0$. This simple model then results in the fact that only a bias-dependent position of the molecular orbitals results in rectification.

The height of the peak at resonance in the differential conductance (in units of G_0) can be approximately given by $\frac{4\lambda}{(1+\lambda)^2}$ which is experimentally close to 10^{-5} demonstrating that $\lambda << 1$.

The differential conductance can then be simplified:

$$\left.\frac{dI(V)}{dV}\right|_{V=V_{1-2}} = 2G_0\lambda\Gamma^2\left[\frac{1+\alpha}{\Gamma^2+4\left(E_0+\frac{V_{1-2}}{2}\times(1+\alpha)\right)^2}+\frac{1-\alpha}{\Gamma^2+4\left(-E_0+\frac{V_{1-2}}{2}\times(1-\alpha)\right)^2}\right] \quad (4)$$

Fitting this expression to the experimental characteristics, the following curve-fitting the parameters $\alpha = -0.19$, $\lambda = 3.8\times10^{-5}$, Γ = 1.31 eV and E_0 = -1.9 eV are obtained. Beyond capturing most of the trends of the experimental curve and accounting for the rectification in the inverse polarization, this minimal model gives a reasonable set of parameters: (1) the position of the molecular level is given below the Fermi level, indicating that the transmission is dominated by the HOMO, and that the HOMO moves ~20% of the applied field, comparable to the dipole matrix element of the HOMO and (2) the ratio between the strongly and weakly coupled lead is $\sim 10^{-5}$, two orders of magnitude between the left and right Hamiltonian matrix elements.

Supporting References

1. Morita, T.; Lindsay, S. Determination of Single Molecule Conductances of Alkanedithiols by Conducting-Atomic Force Microscopy with Large Gold Nanoparticles. *J. Am. Chem. Soc.* **2007**, *129*, 7262.
2. Cigang, X.; Xu, C.; Zalinge, H.; Pearson, J. L.; Glidle, A.; Cooper, J. M.; Cumming, D. R. S.; Haiss, W.; Yao, J.; Schiffrin, D. J.; Proupín-Pérez, M.; *et al*. A Combined Top-Down Bottom-Up Approach for Introducing Nanoparticle Networks Into Nanoelectrode Gaps. *Nanotechnology.* **2006**, 17, 3333.
3. Hegner, M.; Wagner, P.; Semenza, G. Ultralarge Atomically Flat Template-Stripped Au Surfaces for Scanning Probe Microscopy. *Surf. Sci.* **1993**, *291*, 39-46.
4. Stamou, D.; Gourdon, D.; Liley, M.; Burnham, N. A.; Kulik, A.; Vogel, H.; Duschl, C. Uniformly Flat Gold Surfaces: Imaging The Domain Structure of Organic Monolayers using Scanning Force Microscopy. *Langmuir* **1997**, *13*, 2425-2428.
5. Wagner, P.; Hegner, M.; Guntherodt, H. J.; Semenza, G. Formation and in-Situ Modification of Monolayers Chemisorbed on Ultraflat Template-Stripped Gold Surfaces. *Langmuir* **1995**, *11*, 3867-3875.
6. Effenberger, F.; Wurthner, F.; Steybe, F. Synthesis and Solvatochromic Properties of Donor-Acceptor-Substituted Oligothiophenes. *J. Org. Chem.* **1995**, *60*, 2082-2091.